JMEPEG (2011) 20:1638–1641
DOI: 10.1007/s11665-010-9805-z

Preparation and Magnetic Properties of $MnFe_2O_4$ Octahedral Microcrystals

Hua Jiao

(Submitted September 8, 2009; in revised form September 11, 2010)

$MnFe_2O_4$ octahedra have been prepared by reaction of Mn^{2+} ions and Fe^{3+} in alkaline condition via heat treatment of the coprecipitation product. The as-prepared powders were characterized in detail by conventional techniques such as powder x-ray diffraction; field emission electron microscopy and transmission electron microscopy. Vibrating sample magnetometer was used to determine the magnetic properties at room temperature. The results show that the $MnFe_2O_4$ octahedra were single crystals with cubic jacobsite structure and a size distribution from 0.8 to 1.0 μm. The octahedra obtained at 1100 and 1200 °C exhibited a ferromagnetic behavior with the coercive force (H_c) value of 49.03 and 39.23 Oe, saturation magnetization (M_s) value of 42.93 and 47.98 emu/g and remanent magnetization (M_r) value of 2.16 and 2.55 emu/g, respectively. It is indicated that the heat treatment temperature has a significant effect on the formation of the jacobsite structure. Furthermore, a possible mechanism was also proposed to account for the growth of these products.

Keywords coprecipitation, magnetic, $MnFe_2O_4$, octahedra

1. Introduction

$MnFe_2O_4$ is one of the most important magnetic materials, which has a normal spinel structure with tetrahedral A-sites occupied by Mn^{2+} ions and octahedral B-sites by Fe^{3+} ions, which can be expressed as $(Mn^{2+}_{0.8}Fe^{3+}_{0.2})_A\ (Mn^{3+}_{0.2}Fe^{2+}_{0.2}Fe^{3+}_{1.6})_BO_4$ (Ref 1). Nanostructures of $MnFe_2O_4$ have been widely used in electronic applications, contrast-enhancement agents in magnetic resonance imaging (MRI) technology and recording media because of its unique magnetic, optical, chemical and electronic properties (Ref 2, 3). The performance of these devices is mainly due to the ratio of material surface and volume. Normally, the performance is better as the ratio of surface and volume become greater. Therefore, nanostructured $MnFe_2O_4$ has superior performance than the corresponding blocks and is also the basic module to build nanodevices.

In recent years, different kinds of $MnFe_2O_4$ nanostructured materials have been successfully synthesized, such as nanoparticles (Ref 4–11), nanorods (Ref 12, 13) and nanofibers (Ref 14). A TEA-assisted route was normally used to obtain the octahedral-like $MnFe_2O_4$ crystallites (Ref 15). Here, we report a simple route without any assistant for the preparation of $MnFe_2O_4$ octahedra, which were synthesized by reaction of Mn^{2+} ions and Fe^{3+} in alkaline condition, and the influence of heat treatment temperature on magnetism in $MnFe_2O_4$ was investigated. A possible mechanism was also proposed to account for the growth of these products.

2. Experimental Procedures

2.1 Materials

The sample was prepared using the following powder precursors (analytical grade): Fe $(NO_3)_3 \cdot 9H_2O$ and $MnSO_4 \cdot H_2O$ obtained from Tianjing chemical reagent factory and Xi'an chemical reagent factory, respectively. Furthermore, the double-distilled water was used for the aqueous phase.

2.2 Syntheses of $MnFe_2O_4$ Octahedra

In a typical experiment, 16.4 g of Fe $(NO_3)_3 \cdot 9H_2O$ (0.04 mol) was dissolved in 30 mL anhydrous ethanol with continuous stirring about 20 min. Then, 40 mL (0.5 mol/L) of $MnSO_4$ (0.02 mol) was added into the solution. After the solution was stirred for 10 min, the 55 mL (3 mol/L) of NaOH solution was added to form coprecipitation product, which were filtered and washed several times with deionized water and absolute ethanol. Finally, the precipitates were kept at 900, 1000, 1100 and 1200 °C for 1 h, respectively, and then naturally cooled in air.

2.3 Characterization of Products

X-ray powder diffraction (XRD) patterns of the products were obtained on a Japan shimadzu limited XRD-7000 diffractometer at a voltage of 60 kV and a current of 80 mA with Cu Kα radiation ($\lambda = 1.5406$ Å), employing a scanning rate of 8° min^{-1} at the 2θ rang from 20° to 80°. Field emitted scanning electron microscopy (FESEM) images were taken on a JEOL JSM-6700F microscope. Transmission electron microscopy (TEM) images were obtained on a JEOL JEM-3010 transmission electron microscope at an accelerating voltage of 200 kV. Magnetic measurements were carried out at room temperature using a USA Lakeshore 7307 Vibrating sample magnetometer (VSM) with a maximum magnetic field of 10 kOe. The Thermogravimetry (TG) and Differential thermal

Hua Jiao, Department of Chemistry and Chemical Engineering, Weinan Teachers University, Wei Nan 714000, China. Contact e-mail: big7172153@163.com.

analysis (DTA) measurements were simultaneously measured up to 1400 °C at a heating rate of 10 °C/min using a Shanghai ZRY-2P.

3. Results and Discussion

3.1 FESEM analysis

Figure 1(a)-(d) show the FESEM images of the samples which were synthesized by heat treated coprecipitation product at 900, 1000, 1100 and 1200 °C for 1 h, respectively. It can be seen from Fig. 1(a) that the product prepared at 900 °C were reunited particles with size range from 0.4 to 0.5 μm. When the temperature was increased to 1000 °C, the particles grew into octahedral nanostructure with size range about 0.8-1.0 μm, as shown in Fig. 1(b). The octahedral microcrystals with small octahedral particles were obtained, as the temperature increased to 1100 °C (Fig. 1c). After the temperature was increased to 1200 °C, the blocks and small particles were prepared as shown in Fig. 1(d). Moreover, from the inset of Fig. 1(d), there was a fragmented octahedral, which is due to the high temperature. The results indicated that 1100 °C for 1 h was the best reaction condition to the obtain $MnFe_2O_4$ microcrystal.

3.2 XRD Analysis

Figure 2(a)-(d) show the XRD patterns of the samples prepared at 900-1200 °C for 1 h. The peak position and relative intensity of all diffraction peaks for the product match well with standard powder diffraction data. The samples obtained at 900 °C can be indexed to those of the rhombohedra structure of hematite α-Fe_2O_3 (JCPDS card No. 33-0664), orthorhombic structure of bixbyite Mn_2O_3 (JCPDS card No. 24-0508) and cubic structure of manganese iron oxide $(Mn_{0.983}Fe_{0.017})_2O_3$ (JCPDS card No. 24-0507) as shown in Fig. 2(a). It is revealed that $(Mn_{0.983}Fe_{0.017})_2O_3$ was formed from the reaction of Fe_2O_3 and Mn_2O_3. When the temperature was up to 1000 °C, all the diffraction peaks in Fig. 2(b) can be well indexed to $(Mn_{0.983}Fe_{0.017})_2O_3$. After the temperature was increased to 1100-1200 °C, a peak of cubic structure of jacobsite $MnFe_2O_4$ (JCPDS card No. 10-0319) can be observed in Fig. 2(c) and (d). It is indicated that $MnFe_2O_4$ can be obtained at high heat treatment temperature of 1100-1200 °C for 1 h.

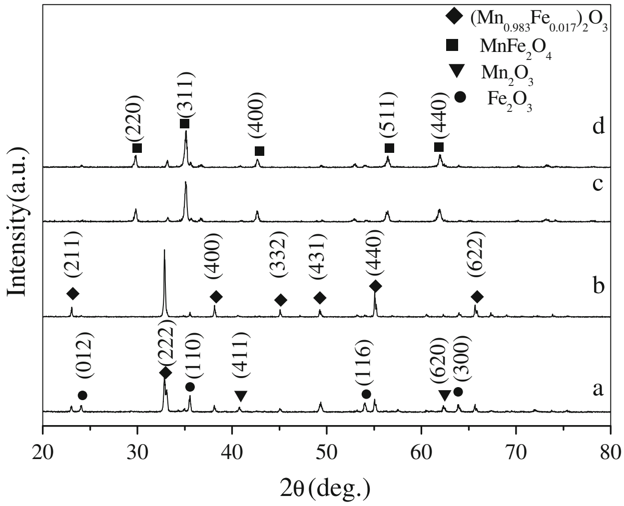

Fig. 2 XRD images of samples obtained at different heat treatment temperatures for 1 h. (a)900 °C; (b) 1000 °C; (c) 1100 °C; (d) 1200 °C

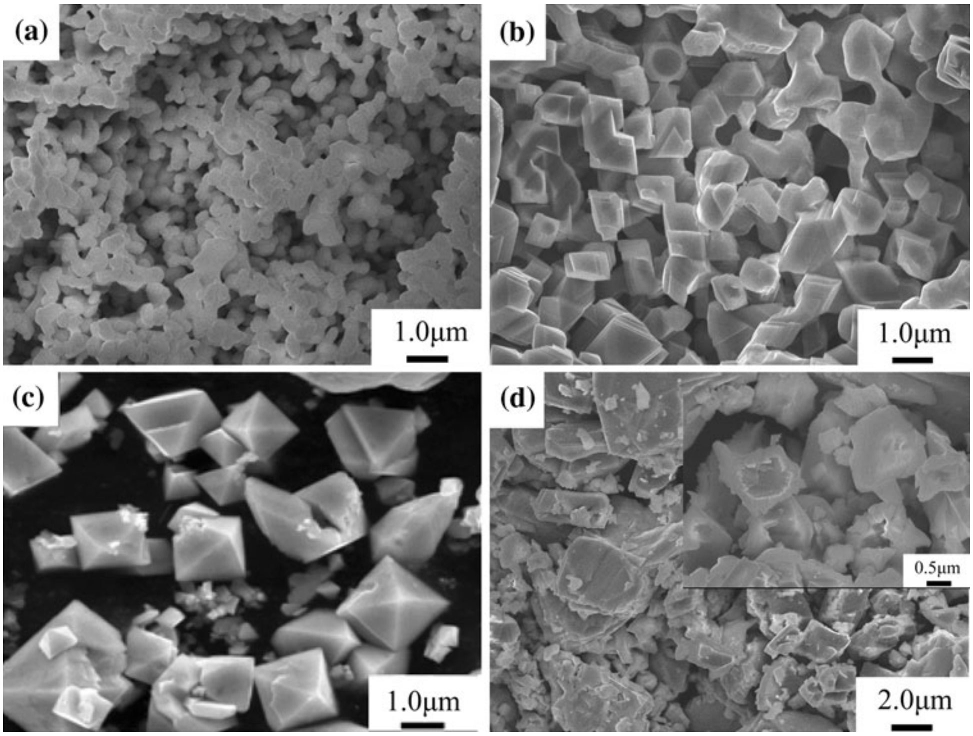

Fig. 1 FESEM images of samples obtained at different heat treatment temperatures for 1 h. (a) 900 °C; (b) 1000 °C; (c) 1100 °C; (d) 1200 °C

3.3 TEM Analysis

The representative TEM image is shown in Fig. 3(a), consistent with those of a sample observed by FESEM in Fig. 1(c). The insets show the sketch images of Fig. 3(a) were electron beam parallel to the [111], [100] and [111] direction of octahedral, respectively. The sizes of the smooth surface octahedral were about 1.0 μm. The SAED pattern taken from a single octahedron can be exactly indexed to a $MnFe_2O_4$ single crystal recorded from the $[\bar{1}11]$ zone axis (Fig. 3b). The SAED and TEM analyses revealed that $MnFe_2O_4$ octahedra were single crystal cubic phase structure.

3.4 Magnetic Measurements

Figure 4(a) and (b) show the magnetic hysteresis curves for the $MnFe_2O_4$ octahedra obtained at 1100 and 1200 °C, respectively. The $MnFe_2O_4$ microcrystal exhibited a weak ferromagnetic behavior with coercivity (H_c) value of 49.03 and 39.23 Oe, remanent magnetization (M_r) value of 2.16 and 2.55 emu/g, saturation magnetization (M_s) value of 42.93 and 47.98 emu/g, which are much smaller than the theoretical values of 120.8 emu/g and bigger than the $MnFe_2O_4$ nanocrystal of 7.8 nm exhibited a low saturation magnetization of 23.9 emu/g. The saturation magnetization of ferrite microcrystal is generally believed to be due to the decreased particles size and presence of a magnetic dead or antiferromagnetic layer on the surface (Ref 7, 15). It is obvious that the magnetic of $MnFe_2O_4$ were increasing as the growth of crystals.

3.5 DTA and TG of $MnFe_2O_4$ Precursor

DTA and TG data (recorded from room temperature to 1400 °C) of the as-synthesized precursor recorded simultaneously at a rate of 10 °C/min were shown in Fig. 5. The DTA pattern shows a small endothermic transformation between room temperature and 80 °C. This endothermic peak was accompanied by a weight loss of ~11% in the TG curve which was attributed to the loss of a small quantity of ethanol adsorbed on the solid surface of the as-prepared sample, which did not remove even after room temperature drying (Ref 16). An exothermic peak centered at 700 °C in DTA which accompanied by a weight loss of ~33% in the TG curve could

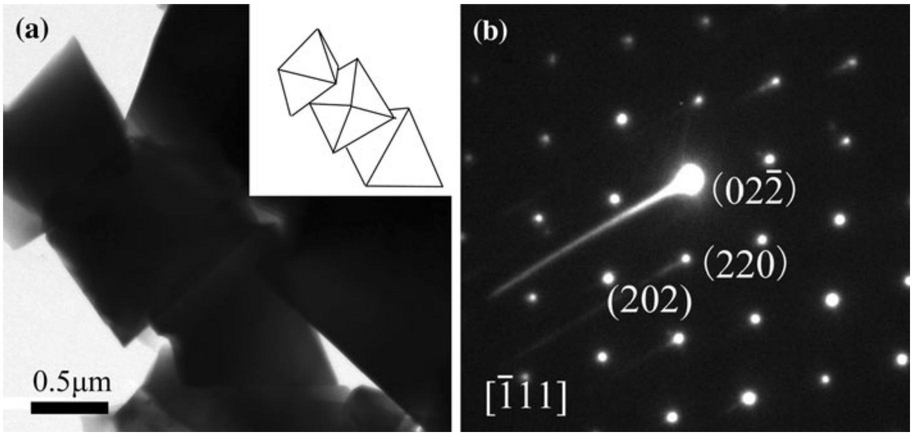

Fig. 3 TEM images of samples obtained at 1100 °C for 1 h. (a) TEM; (b) SAED

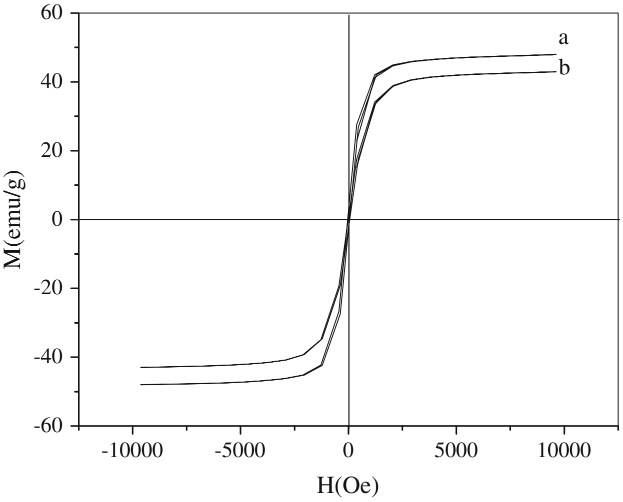

Fig. 4 Magnetic hysteresis curves measured at room temperature for $MnFe_2O_4$ octahedra heat treatment at 1100 °C (a) and 1200 °C (b) for 1 h

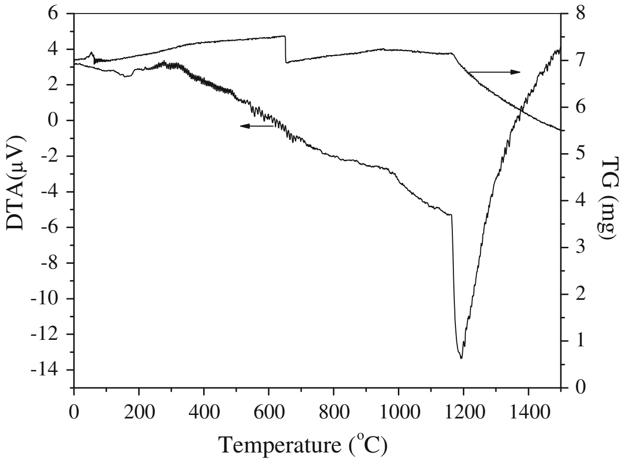

Fig. 5 DTA/TG of the $MnFe_2O_4$ precursor obtained at a heating rate of 10 °C/min

be observed. This can be attributed to the decomposing a mount of $Fe(OH)_3$ and $Mn(OH)_2$ precipitates. Moreover, a strong exothermic peak at 1100-1200 °C in DTA was accompanied by a weight loss in the TG curve. It is indicated that $MnFe_2O_4$ can be obtained from Mn_2O_3 and Fe_2O_3. In this paper, DTA-TG as well as the heat treatment of the precursor was carried out in the presence of air atm and the O_2, which decomposed from the reaction of Fe_2O_3 and Mn_2O_3 might result in a strong exothermic peak at 1100-1200 °C.

3.6 Mechanism Analysis of Synthesis

The experiment results revealed that $MnFe_2O_4$ octahedra can be obtained via heat treatment of coprecipitation product, which were synthesis by reaction of Mn^{2+} ions and Fe^{3+} ions in alkaline condition. The $MnFe_2O_4$ formation proceeds may be as follows: first, Mn^{2+} and Fe^{3+} ions reacted to OH^- in aqueous ethanol solution formed $Fe(OH)_3$ and $Mn(OH)_2$ coprecipitation product, respectively (Eq 1, 2); Subsequently, the obtained $Fe(OH)_3$ and $Mn(OH)_2$ deposition dehydrate into Fe_2O_3 and Mn_2O_3 (Eq 3, 4). Finally, $MnFe_2O_4$ can be prepared via the reaction of Fe_2O_3 and Mn_2O_3 (Eq 5). The chemical reaction can be expressed as:

$$Mn^{2+} + 2OH^- \rightarrow Mn(OH)_2 \downarrow \qquad \text{(Eq 1)}$$

$$Fe^{3+} + 3OH^- \rightarrow Fe(OH)_3 \downarrow \qquad \text{(Eq 2)}$$

$$4Mn(OH)_2 + O_2 \xrightarrow{\Delta} 2Mn_2O_3 + 4H_2O \qquad \text{(Eq 3)}$$

$$2Fe(OH)_3 \xrightarrow{\Delta} Fe_2O_3 + 3H_2O \qquad \text{(Eq 4)}$$

$$2Mn_2O_3 + 4Fe_2O_3 \xrightarrow{\Delta} 4MnFe_2O_4 + O_2 \uparrow \qquad \text{(Eq 5)}$$

In this process, the coprecipitation reaction of Eq 3 and 4 lead reversible reactions of Eq 1 and 2 towards right direction. Finally, we obtained $MnFe_2O_4$ octahedra via heat treatment of coprecipitation products in high temperature condition.

The shapes of $MnFe_2O_4$ octahedra were dependent on the formation of nucleus and its growth speed in different directions. It is believed that the absence of anhydrous ethanol can reduce the formation speed of $Fe(OH)_3$ nucleus and growth. At first, $[Fe(H_2O)]_6^{3+}$ molecules were adsorbed by anhydrous ethanol, which can reduce the growth speed of [111] direction. The resulting of formation octahedron shapes due to the growth speed of [100], [010] and [001] direction was equally and the ratio of {100} to {111} was 1.73 (Ref 17).

4. Conclusions

In summary, $MnFe_2O_4$ octahedra have been successfully prepared via heat treatment of coprecipitation products without any assistant. Moreover, the influence of heat treatment temperature on magnetism of $MnFe_2O_4$ octahedra was investigated. A possible mechanism was also proposed to account for the growth of these samples. These $MnFe_2O_4$ octahedra have potential applications in design of nanoscale devices, ultrahigh-density magnetic storage devices and biomedicine for targeted drug delivery fields.

Acknowledgment

This work was supported by the Fund of Weinan Teachers University (10YKF014).

References

1. G. Bonsdorf, M.A. Denecke, K. Schäfer, S. Christen, H. Langbein, and W. Gunßer, X-ray Absorption Spectroscopic and Mossbauer Studies of Redox and Canon-Ordering Processes in Manganese Ferrite, *Solid State Ionics*, 1997, **101–103**, p 351–357
2. Y. Torii, A. Tsuzuki, K. Kato, Y. Uwamino, B.H. Choi, and M.J. Lee, Chemical Processing and Characterization of Spinel-Type Thermistor Powder in the Mn-Ni-Fe Oxide System, *J. Mater. Sci.*, 1996, **31**, p 2603–2607
3. Z. Šimša, P. Thailhades, L. Presmanes, and C. Bonningue, Magneto-Optical Properties of Manganese Ferrite Films, *J. Magn. Magn. Mater.*, 2002, **242–245**, p 381–383
4. W.W. Wang, Microwave-Induced Polyol-Process Synthesis of $M^{II}Fe_2O_4$ (M = Mn, Co) Nanoparticles and Magnetic Property, *Mater. Chem. Phys.*, 2008, **108**, p 227–231
5. U.I. Tromsdorf, N.C. Bigall, M.G. Kaul et al., Size and Surface Effects on the MRI, Relaxivity of Manganese Ferrite Nanoparticle Contrast Agents, *Nano Lett.*, 2007, **7**, p 2422–2427
6. X.M. Liu, G. Yang, and S.Y. Fu, Mass synthesis of Nanocrystalline Spinel Ferrites by a Polymer-Pyrolysis Route, *Mater. Sci. Eng. C*, 2007, **27**, p 750–755
7. N.Z. Bao, L.M. Shen, Y. Wang, P. Padhan, and A. Gupta, A Facile Thermolysis Route to Monodisperse Ferrite Nanocrystals, *J. Am. Chem. Soc.*, 2007, **129**, p 12374–12375
8. Q. Song, Y. Ding, Z.L. Wang, and Z.J. Zhang, Tuning the Thermal Stability of Molecular Precursors for the Nonhydrolytic Synthesis of Magnetic $MnFe_2O_4$ Spinel Nanocrystals, *Chem. Mater.*, 2007, **19**, p 4633–4638
9. H. Zeng, M.R. Philip, A.X. Wang, and S.H. Sun, Shape-Controlled Synthesis and Shape-Induced Texture of $MnFe_2O_4$ Nanoparticles, *J. Am. Chem. Soc.*, 2004, **126**, p 11458–11459
10. C.R. Sun, S.H.L. Jerry, and M.Q. Zhang, Magnetic Nanoparticles in MR Imaging and Drug Delivery, *Adv. Drug Deliv. Rev.*, 2008, **60**, p 1252–1265
11. J. Hu, M.C.L. Irene, and G.H. Chen, Fast Removal and Recovery of Cr(VI) Using Surface-Modified Jacobsite ($MnFe_2O_4$) Nanoparticles, *Langmuir*, 2005, **21**, p 11173–11179
12. L. Zhen, K. He, C.Y. Xu, and W.Z. Shao, Synthesis and Characterization of Single-Crystalline $MnFe_2O_4$ Nanorods via a Surfactant-Free Hydrothermal Route, *J. Magn. Magn. Mater.*, 2008, **320**, p 2672–2675
13. J. Wang, Q.W. Chen, B.Y. Hou, and Z.M. Peng, Synthesis and Magnetic Properties of Single-Crystals of $MnFe_2O_4$ Nanorods, *Eur. J. Inorg. Chem.*, 2004, **35**, p 1165–1168
14. Y.W. Ju, J.H. Park, H.R. Jung, S.J. Cho, and W.J. Lee, Electrospun $MnFe_2O_4$ Nanofibers: Preparation and Morphology, *Compos. Sci. Technol.*, 2008, **68**, p 1704–1709
15. D.E. Zhang, X.J. Zhang, X.M. Ni, J.M. Song, and H.G. Zheng, Low-Temperature Fabrication of $MnFe_2O_4$ Octahedrons: Magnetic and Electrochemical Properties, *Chem. Phys. Lett.*, 2006, **426**, p 120–123
16. M. Sivakumar, T. Takami, H. Ikuta, A. Towata, K. Yasui, T. Tuziuti, T. Kozuka, D. Bhattacharya, and Y. Iida, Fabrication of Zinc Ferrite Nanocrystals by Sonochemical Emulsification and Evaporation: Observation of Magnetization and Its Relaxation at Low Temperature, *J. Phys. Chem. B*, 2006, **110**, p 15234–15243
17. Z.L. Wang, Transmission Electron Microscopy of Shape-controlled Nanocrystals and Their Assemblies, *J. Phys. Chem. B*, 2000, **104**, p 1153–1175